Research Article

For reprint orders, please contact: reprints@futuremedicine.com

Nanomedicine

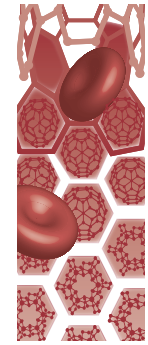

Zinc oxide nanoparticles impair bacterial clearance by macrophages

Aim: The extensive development of nanoparticles (NPs) and their widespread employment in daily life have led to an increase in environmental concentrations of substances that may pose a biohazard to humans. The aim of this work was to examine the effects of zinc oxide nanoparticles (ZnO-NPs) on the host's pulmonary immune system response to nontypeable Haemophilus influenzae (NTHi) infection. **Materials & Methods:** A murine infection model was employed to assess pulmonary inflammation and bacterial clearance in response to exposure to ZnO-NPs. The molecular mechanisms underlying ZnO-NP-impaired macrophage activation were investigated. **Results:** Treatment with ZnO-NPs impaired macrophage activation, leading to a delay in NTHi clearance in the bronchial alveolar lavage fluids and lungs. Exposure to ZnO-NPs followed by NTHi challenge decreased levels of nitric oxide compared with NTHi infection alone. The effects of ZnO-NPs involved downregulation of NTHi-activated expression of inducible nitric oxide synthase and the translocation of active NF-kB into the nucleus. **Conclusion:** These results demonstrate that exposure to ZnO-NPs can impair innate immune responses and attenuate macrophage responses to bacterial infection.

Original submitted 17 December 2013; Revised submitted 3 March 2014

Keywords: bronchial alveolar lavage fluid • macrophage • nitric oxide • nontypeable *Haemophilus influenzae* • zinc oxide nanoparticles

Chia-Der Lin[1], Yu-Yi Kou[2], Chin-Yu Liao[2], Ching-Hao Li[3], Shiao-Ping Huang[4], Yu-Wen Cheng[5], Wei-Chih Liao[6], Hao-Xiang Chen[2], Pei-Ling Wu[7], Jaw-Jou Kang[8], Chen-Chen Lee*[,2] & Chih-Ho Lai*[,2]

[1]Department of Otolaryngology-Head & Neck Surgery, China Medical University Hospital, Taichung, Taiwan
[2]Department of Microbiology & Graduate Institute of Basic Medical Science, China Medical University, Taichung, Taiwan
[3]Department of Physiology, School of Medicine, Taipei Medical University, Taipei, Taiwan
[4]Department of Medical Laboratory Science & Biotechnology, Fooyin University, Kaohsiung, Taiwan
[5]School of Pharmacy, Taipei Medicine University, Taipei, Taiwan
[6]Department of Pulmonary & Critical Care Medicine, China Medical University Hospital, Taichung, Taiwan
[7]Department of Cosmeceutics, China Medical University, Taichung, Taiwan
[8]Graduate Institute of Toxicology, College of Medicine, National Taiwan University, Taipei, Taiwan
*Authors for correspondence:
Chen-Chen Lee
Tel.: +886 4 22052121 ext. 7706
Fax: +886 4 22333641
leechenchen@mail.cmu.edu.tw
Chih-Ho Lai
Tel.: +886 4 22052121 ext. 7729
Fax: +886 4 22333641
chl@mail.cmu.edu.tw

Nanoparticles (NPs) are defined as particles with a diameter smaller than 100 nm that have been used widely in human living environments [1]. Nanomaterials employed in products are easily adsorbed by and penetrate into biological systems, posing a health risk to humans [2,3]. As the use of NPs increases, the possible toxic effects on human health have raised serious concerns [4,5].

In recent years, zinc oxide nanoparticles (ZnO-NPs) have been synthesized and are frequently included in commonly used products, including sunscreens, cosmetic products, food and medical materials [6–9]. Application of sunscreens containing ZnO-NPs might result in their absorption through the skin and the appearance of elevated levels of Zn in the blood and urine [10,11]. However, several studies suggest that metal oxide nanoparticles can lodge in hair follicles, sweat glands or skin folds but not penetrate through the skin [12,13]. It has been reported that oral administration and intraperitoneal injection of ZnO-NPs resulted in Zn absorption into the circulatory system, followed by biodistribution to the liver, spleen and kidney [14]. Exposure to uncoated ZnO-NPs may mitigate the cellular responses in human olfactory cells with varying degrees [15]. In addition, ZnO-NPs have been reported to play a role in pathogenesis in endothelial inflammation associated with cardiovascular diseases [16]. NPs possess well-known antimicrobial activity [17], and their influence on human immune/inflammatory responses has also been reported [18,19]. However, the toxicological relevance of ZnO-NPs in the respiratory airway, especially with respect to host

Future Medicine part of fsg

defense against bacterial infection, currently remains uncharacterized.

Haemophilus influenzae, a Gram-negative coccobacillus with a pleomorphic shape, belongs to the flora that normally colonize the human upper respiratory tract [20]. Strains without a polysaccharide capsule are designated as nontypeable *H. influenzae* (NTHi), and are the main cause of *Haemophilus* respiratory infections [21]. A large number of respiratory diseases arise from NTHi infection, including otitis media with effusion, bronchitis, pneumonia, and chronic obstructive pulmonary disease (COPD) [22–25]. Deficient pulmonary immune responses may lead to acute exacerbation of chronic airway inflammation by NTHi [26].

The aim of this study was to explore whether ZnO-NPs affect the host pulmonary immune system's response to NTHi infection. We established a nanoparticle-exposed mouse model that was challenged with NTHi to evaluate pulmonary immune responses and lung bacterial clearance. Additional studies were then carried out to investigate the effect of ZnO-NPs on triggering signaling molecules and modulating inflammasome activation, which may lead to attenuation of pulmonary immune activation in response to NTHi infection.

Materials & methods

Preparation & characterization of nanoparticles

Zinc oxide nanoparticles (ZnO-NPs) and zinc oxide microparticles (ZnO-MPs) were obtained from Jaw-Jou Kang (Graduate Institute of Toxicology, National Taiwan University, Taiwan) [14]. The particle sizes and physicochemical characteristics of ZnO-NPs and ZnO-MPs were determined by TEM (JEM-1200EX II TEM, Jeol, Japan) and dynamic light scattering (DLS; Zetasizer Nano series, Malvern Instruments Ltd, UK). The concentration of the particles that was used to characterize the physicochemical characteristics is 10 μg/ml in phosphate-buffered saline (PBS) or RPMI containing 10% FBS. As shown in Table 1, the diameters of ZnO-NPs were approximately 50 nm, and ZnO-MPs with external diameters were more than 100 nm [14,16]. The intensity-weight average hydrodynamic diameters of ZnO-NPs and ZnO-MPs were 93 ± 14 nm and 1226 ± 120 nm, respectively (Supplementary Figure 2; see online at http://www.futuremedicine.com/doi/full/10.2217/NNM.14.48). The particle suspensions were prepared using DMSO at 1, 5 and 10 μg/ml followed by sonication for 10 min and immediate application to cell experiments.

Inductively coupled plasma-mass spectrometry assay

The concentration zinc ion in RPMI medium containing 10% FBS was detected by inductively coupled plasma-mass spectrometry (ICP-MS; Element, Finnigan MAT, Germany), as described previously [14]. Briefly, different concentrations of particles were incubated in RPMI medium containing 10% FBS for 3 h. The medium was collected for centrifuging at 10000 ×*g*. The supernatant was then prepared to analyze the zinc ion concentration by ICP-MS.

Reagents & antibodies

Antibodies against inducible nitric oxide synthase (iNOS) and cyclooxygenase 2 (COX-2) were purchased from Santa Cruz Biotechnology (CA, USA). NF-κB-Luc plasmids were purchased from Stratagene (CA, USA). The pSV-β-galactosidase vector and the luciferase assay kit were purchased from Promega (WI, USA). All other reagents were obtained from Sigma-Aldrich (MO, USA).

Animals & experimental protocol

C57BL/6 mice aged 6 weeks from the National Laboratory Animal Center (Tainan, Taiwan) were employed in this study. All procedures were manipulated in compliance with the Animal Care and Use Guidelines for the China Medical University under a protocol approved by the Institutional Animal Care Use Committee. The experimental protocol was designed and is shown in Figure 1A. Briefly, mice were divided into ten groups (five mice each) and exposed or sham exposed to particles (ZnO-NPs or ZnO-MPs) by micropump nebulizer

Table 1. Physiochemical characterization of zinc oxide nanoparticles and zinc oxide nanoparticles in dry, aqueous and cell culture medium.

Particle	Particle size (nm)†	Particle size (nm) (DLS)‡		Zeta potential (mV)	
		PBS	RPMI	PBS	RPMI
ZnO-MPs	2741 ± 315	1226 ± 120	726 ± 80	-8.8 ± 0.7	-7.7 ± 0.7
ZnO-NPs	46 ± 7	93 ± 14	91 ± 7	-7.4 ± 0.4	-8.5 ± 0.4

The concentration of particles that are used for DLS is 10 μg/ml. Results represent the mean ± standard deviation values for three independent experiments.
†Particle size was measured by TEM.
‡The size distribution and zeta potential of the particles were determined by DLS.
DLS: Dynamic light scattering; PBS: Phosphate-buffered saline; pH7.4; RPMI: Culture medium containing 10% FBS, pH7.4; ZnO-MP: Zinc oxide microparticle; ZnO-NP: Zinc oxide nanoparticle.

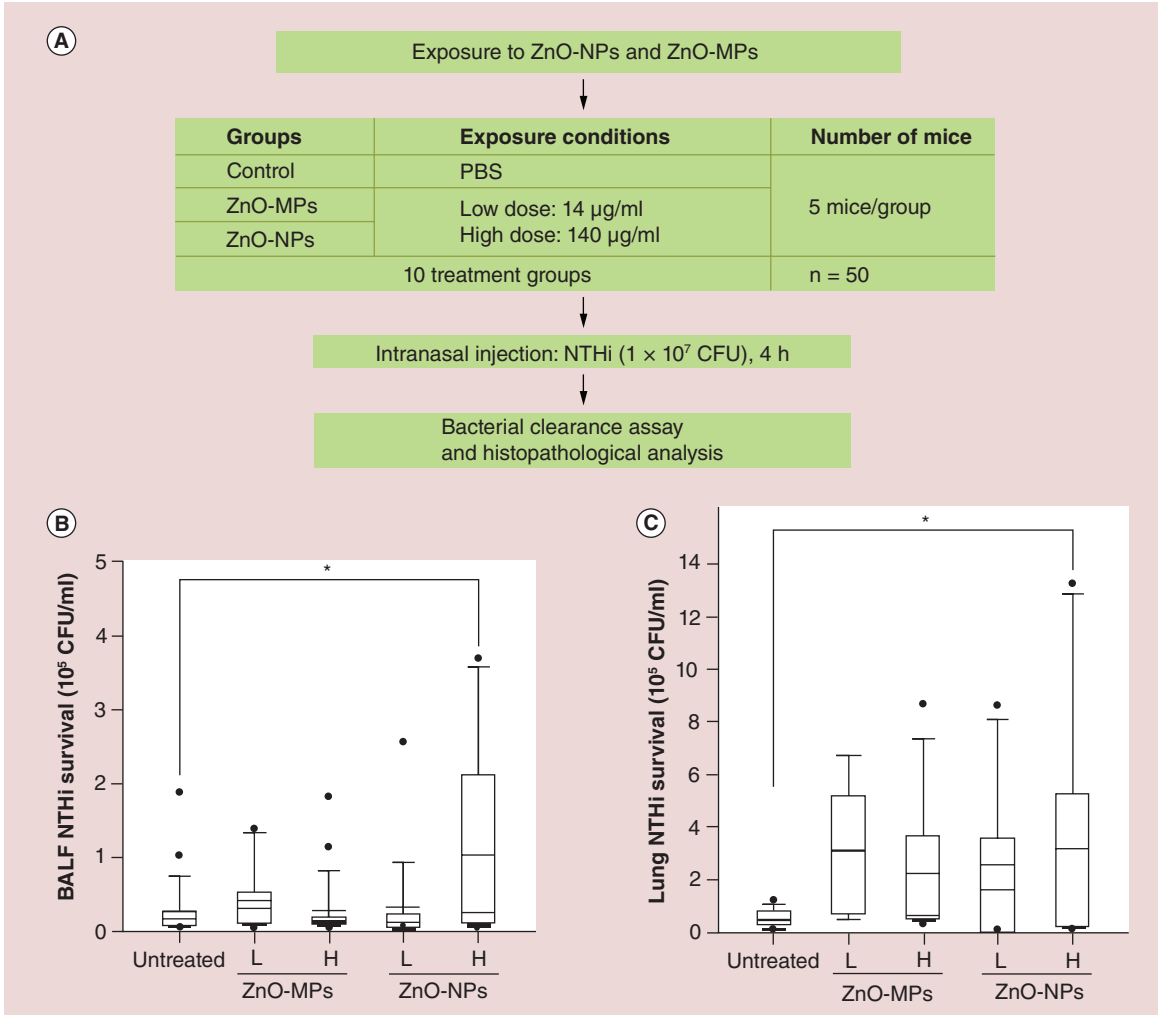

Figure 1. Zinc oxide nanoparticles enhance nontypeable *Haemophilus influenzae* survival in murine pulmonary tissues. **(A)** The mice were exposed to zinc oxide nanoparticles or zinc oxide nanoparticles for 2 weeks under various conditions: untreated (sham-exposed to particles), low particle doses (L; 14 µg/ml) or high particle doses (H; 140 µg/ml). 4 h after infection with nontypeable *Haemophilus influenzae*, the mice were sacrificed and levels of nontypeable *Haemophilus influenzae* surviving in **(B)** bronchoalveolar lavage fluid and **(C)** lung tissues were estimated, as described in the 'Materials & methods' section. Summary statistics for the distribution of the data are shown using box plots. The ends of the boxes define the 25th and the 75th percentiles. The outlier values (between 1.5 and 3.0 box lengths) are shown with closed circles. Red lines in the boxes indicate the average, and black lines represent the median. All groups were compared with an untreated group and significance was assessed using the Student's *t*-test.
*$p < 0.05$.
CFU: Colony-forming units; H: High particle doses (140 µg/ml); L: Low particle doses (14 µg/ml); NTHi: Nontypeable *Haemophilus influenzae*; PBS: Phosphate-buffered saline; ZnO-MP: Zinc oxide microparticle; ZnO-NP: Zinc oxide nanoparticle.

(Aerogen, Galway, Ireland) at a high dose (140 µg/ml) or low dose (14 µg/ml) once per day for two consecutive weeks, respectively. The particle exposure doses were dissolved in PBS followed by sonication and immediately applied to mice. Mice were placed in chambers and were exposed to 10 ml of different doses of particles for 30 min. Mice were then infected or uninfected with NTHi (1×10^7 CFU) by intranasal injection and sacrificed at 4 h postinfection. The bronchoalveolar lavage fluid (BALF) and isolated lung were collected as described previously [27,28]. Wright–Giemsa Stain (Sigma-Aldrich) was used to classify the inflammatory cells. The analyses of cytokine secretions and bacterial clearance in BALF were then performed. Lungs were isolated from mice and fixed with 10% neutral phosphate-buffered formalin (Sigma-Aldrich). The tissue sections were prepared and stained with hematoxylin/eosin (H&E). The stained samples were observed and scored using a microscope (Carl Zeiss, Göttingen, Germany). Each specimen was selected using ten vision fields to determine the inflammatory infiltration. The inflammatory responses were evaluated [29]: score 0 – normal lung tissue; score 1 –

slight inflammation; score 2 – moderate inflammation; score 3 – severe inflammation.

Cell & bacterial cultures

RAW264.7 cells (ATCC TIB-71) were cultured in RPMI-1640 medium (HyClone, UT, USA) containing 10% complement-inactivated fetal bovine serum (HyClone). The cells were maintained at 37°C in a humid atmosphere containing 5% CO_2. The culture medium was not supplemented with antibiotics upon bacterial infection experiments. Nontypeable *H. influenzae* (NTHi, ATCC 49247) were routinely cultured on chocolate agar (Becton Dickinson, MD, USA) supplemented with 10 µg/ml hemin and 10 µg/ml β-nicotinamide adenine (NAD; Sigma-Aldrich) [30]. The NTHi were incubated under 5% CO_2 and 10% O_2 conditions at 37°C for 24 h, and stocked at 4°C before the experiments.

Cytotoxicity assay

The cell viability assay was used to measure the cytotoxicity of ZnO-NPs in RAW264.7 cells as described previously [31]. Briefly, cells (2×10^4) were seeded in a 96-well culture plate followed by treatment with ZnO-NPs or ZnO-MPs at concentrations of 1, 5, 10 µg/ml (0.26, 1.3, 2.6 ☒g/cm^2) for 24 h. Cells were treated with 200 µg/ml 1-(4,5-dimethylthiazol-2-yl)-3,5-diphenylformazan (MTT; Sigma-Aldrich) and incubated for 3 h. Cell viability was measured by the ability of viable cells to reduce MTT (Sigma-Aldrich) to formazan.

Bactericidal assay

NTHi suspensions were adjusted to 0.2 with optical density (OD) at 600 nm and treated with ZnO-NPs or ZnO-MPs at concentrations of 10^0, 10^1, 10^2 and 10^3 µg/ml. The treated bacteria were incubated at 37°C for 24 h and cultured by serial dilution onto chocolate agar. After 24-h incubation, colony-forming units (CFU) were counted to determine bactericidal activity.

Measurement of cytokines

The supernatants from cell cultures were collected, and the levels of keratinocyte-derived chemokines (KCs), IL-6 and TNF-α were determined by using a sandwich ELISA kit (R&D Systems, MN, USA) [32].

Table 2. PCR primers that were used in this study.

Gene	Primer	Nucleotide sequence (5′–3′)
iNOS	Forward	CCCAGAGTTCCAGCTTCTGG
	Reverse	CCAAGCCCCTCACCATTATCT
COX-2	Forward	GAAGTCTTTGGTCTGGTGCCTG
	Reverse	GTCTGCTGGTTTGGAATAGTTGC
GAPDH	Forward	CTCAACTACATGGTCTACATGTTCCA
	Reverse	CTCAACTACATGGTCTACATGTTCCA

Phagocytosis assay

RAW264.7 cells (5×10^5) were cultured on a 24-well plate for 24 h followed by treatment with ZnO-NPs. The cells were then infected with NTHi for further 3 h at a multiplicity of infection (MOI) of 100. To determine the number of extracellular NTHi, the infected cells were washed with PBS to remove unbound bacteria and then lysed with distilled water for 10 min. Lysates were diluted in PBS, plated onto chocolate agar plates and cultured for 24 h, after which the colony-forming units (CFU) were counted. To determine the number of viable intracellular bacteria, NTHi-infected cells were washed three times with PBS and incubated with gentamicin (100 µg/ml) for 1 h to remove extracellular bacteria [33]. The treated samples were followed by the same procedures to determine the number of CFU.

Phagocytosis assay was performed by using fluorescein isothiocyanate (FITC)-conjugated NTHi. NTHi (5×10^8) were heat killed at 95°C for 5 min. Heat-killed bacteria were incubated with 0.5 mg/ml FITC in 0.1 M carbonate buffer (pH9.0). The FITC-conjugated NTHi were washed three times and suspended in PBS. Macrophages were treated with ZnO-NPs and then incubated for 3 h with FITC-conjugated NTHi. The cells were washed and suspended in PBS containing 0.2% trypan blue to quench fluorescence, which was caused by the binding of bacteria to the surface of cells. Phagocytic activity was determined by flow cytometry (Becton Dickinson, CA, USA) and expressed as the mean fluorescence intensity (MFI) analyzed by Cell Quest software WinMDI (Verity Software House, ME, USA).

Determination of nitric oxide

RAW264.7 cells (5×10^5) were cultured in 24-well plate for 24 h and treated with ZnO-NPs for 3 h prior to infection with NTHi for 3 h at an MOI of 100. The culture medium was collected and the NO production was determined by using Griess Reagents (Sigma-Aldrich) [34].

Reverse transcription & quantitative real-time PCR

RAW264.7 cells (5×10^5) were cultured in a 24-well plate for 24 h and treated with ZnO-NPs for 3 h prior to infection with NTHi for 3 h at an MOI of 100. Total RNA was prepared from ZnO-NP-treated and/or NTHi-infected cells using REzol (PROtech Technologies, Taipei, Taiwan). Total RNA (2 µg) was reverse transcribed into cDNA using the oligo(dT) primer. Quantitative real-time PCR using SYBR Green I Master Mix and a model 7900 Sequence Detector System

(Applied Biosystems, CA, USA) was conducted as described previously [35]. The oligonucleotide primers for PCR amplification of murine iNOS, COX-2 and GAPDH are shown in Table 2. The PCR program was performed at 50°C for 2 min with 40 cycles of 95°C for 10 s and 60°C for 1 min. The threshold was set above the non-template control background and within the linear phase of target gene amplification in order to calculate the cycle number at which the transcript was detected (denoted as C_T).

Western blot analysis

RAW264.7 cells (1×10^6) were cultured in a six-well plate for 24 h and treated with ZnO-NPs for 3 h prior to infection with NTHi for 3 h at an MOI of 100. The prepared cells were washed three times and boiled with SDS-PAGE sample buffer (62.5 mM Tris-HCl [pH 6.8], 2% SDS, 10% glycerol, 0.05% brilliant blue R) at 100°C for 10 min. The samples were then resolved by 10% SDS-PAGE and transferred onto polyvinylidene difluoride membranes (Millipore, MA, USA). The membranes were blocked by 5% skim milk in PBST (PBS buffer containing 0.1% Tween 20) at 4°C overnight and then incubated with the first antibodies against COX-2 (dilution 1:2000) and β-actin (dilution 1:10,000) at 4°C overnight. The membranes were then incubated with HRP-conjugated secondary antibodies (Millipore) at a dilution of 1:4000. The proteins of interest were visualized by using the ECL™ Western Blotting Detection Reagents (RE Healthcare, UK) and were detected using ImageQuant LAS-4000 (GE Healthcare, WI, USA).

NF-κB reporter luciferase assay

RAW264.7 cells were plated in a 12-well plate and then transfected with a NF-κB-luc reporter plasmid (1 μg) using Lipofectamine 2000 (Invitrogen), as described previously [36]. The transfected cells were lysed, and luciferase assays were performed with the Dual-Luciferase Reporter Assay System and normalized by co-transfection with a β-galactosidase expression vector (Promega, MA, USA).

Immunofluorescence staining of phosphorylated p65

RAW264.7 cells were cultured on coverslips then treated with or without ZnO-NPs for 3 h followed by infection with or without NTHi for an additional 3 h. Cells were fixed, permeabilized and probed with anti-p65 (H-286; Santa Cruz Biotechnology). Cells were then incubated with a secondary antibody, Alexa Fluor® 488-conjugated goat anti-mouse IgG (Invitrogen, CA, USA) and propidium iodide (Calbiochem, CA, USA). The nuclear translocation of phosphorylated p65 was observed by a confocal laser scanning microscope (Zeiss LSM 510, Carl Zeiss, Göttingen, Germany). The quantification of fluorescence intensity was performed by ImageJ [34].

Statistical analysis

A Student's *t*-test and one way ANOVA was employed to calculate the statistical significance of the experimental results between two groups; a p-value less than 0.05 was considered significant.

Results

ZnO-NPs enhance NTHi survival in a murine model of pulmonary infection

We first examined the effects of various concentrations of zinc oxide nanoparticles (ZnO-NPs) and zinc oxide microparticles (ZnO-MPs) on bacterial clearance in a murine model of pulmonary infection (Figure 1A). Mice were exposed to different concentrations of ZnO-NPs or ZnO-MPs for 14 days, and were sacrificed 4 h postinfection with NTHi. The number of bacteria remaining in the BALFs and lungs was then assessed. Upon exposure to high concentrations (140 μg/ml) of ZnO-NPs, NTHi survival increased significantly not only in the BALFs, but also in the lungs (Figure 1B). However, bacterial viability was not affected in mice treated with low concentrations (14 μg/ml) of ZnO-NPs or varying concentrations (14 or 140 μg/ml) of ZnO-MPs. These data indicate that inhalation of high concentrations of ZnO-NPs reduce bacterial clearance but does not affect bacterial viability in the lungs.

ZnO-NPs impair macrophage activation

Cell differentiation was then examined in murine BALFs. As shown in Figure 2A, BALF cells significantly increased in number 4 h postinfection with NTHi when compared with noninfected controls. Upon murine exposure to ZnO-NPs followed by infection with NTHi, levels of BALF cells remained high. We then analyzed cell differentiation of infiltrated inflammatory cells in BALFs. Our data showed that regardless of whether they were treated with ZnO-NPs, the numbers of BALF cells, neutrophils, eosinophils and activated macrophages elevated dramatically after infection with NTHi (Figure 2B–D). However, the levels of activated macrophages decreased significantly after exposure to high concentrations of ZnO-NPs and infection with NTHi compared with the group not treated with NPs (Figure 2D). We also detected the effects of ZnO-MPs on BALF cells. As shown in Supplementary Figure 3, ZnO-MPs did not clearly affect the BALF cell profiles among the NTHi-treated groups.

Lung tissues isolated from mice were stained with H&E to evaluate levels of infiltrated inflammatory

cells. As shown in Figure 3A, inflammatory cell infiltration was absent in lung tissue from mice that were not infected with NTHi or were treated with ZnO-NPs. After infection with NTHi, levels of lung inflammation in mice significantly increased. However, lung inflammatory responses showed no obvious change when mice were exposed to ZnO-NPs prior to challenge with NTHi (Figure 3B).

ZnO-NPs suppress inflammatory mediator production in BALFs in response to bacterial infection

To investigate the effect of ZnO-NPs on the production of inflammatory mediators/cytokines in BALFs in response to NTHi infection, mice were exposed to ZnO-NPs and then challenged with NHTi for 4 h. After pretreatment with ZnO-NPs alone, the mice showed negligible responses in cytokine secretions, including TNF-α, KC and IL-6 (Figure 4A–C). Infection of mice with NTHi resulted in elevated levels of all cytokines tested, similar to those of mice treated with ZnO-NPs and NTHi. Although the level of nitric oxide (NO) was undetectable, mRNA expression of inducible nitric oxide synthase (iNOS) increased markedly in the NTHi-infected group compared with the uninfected group (Figure 4D). In comparison with NTHi infection alone, mice exposed to ZnO-NPs and then infected with NTHi

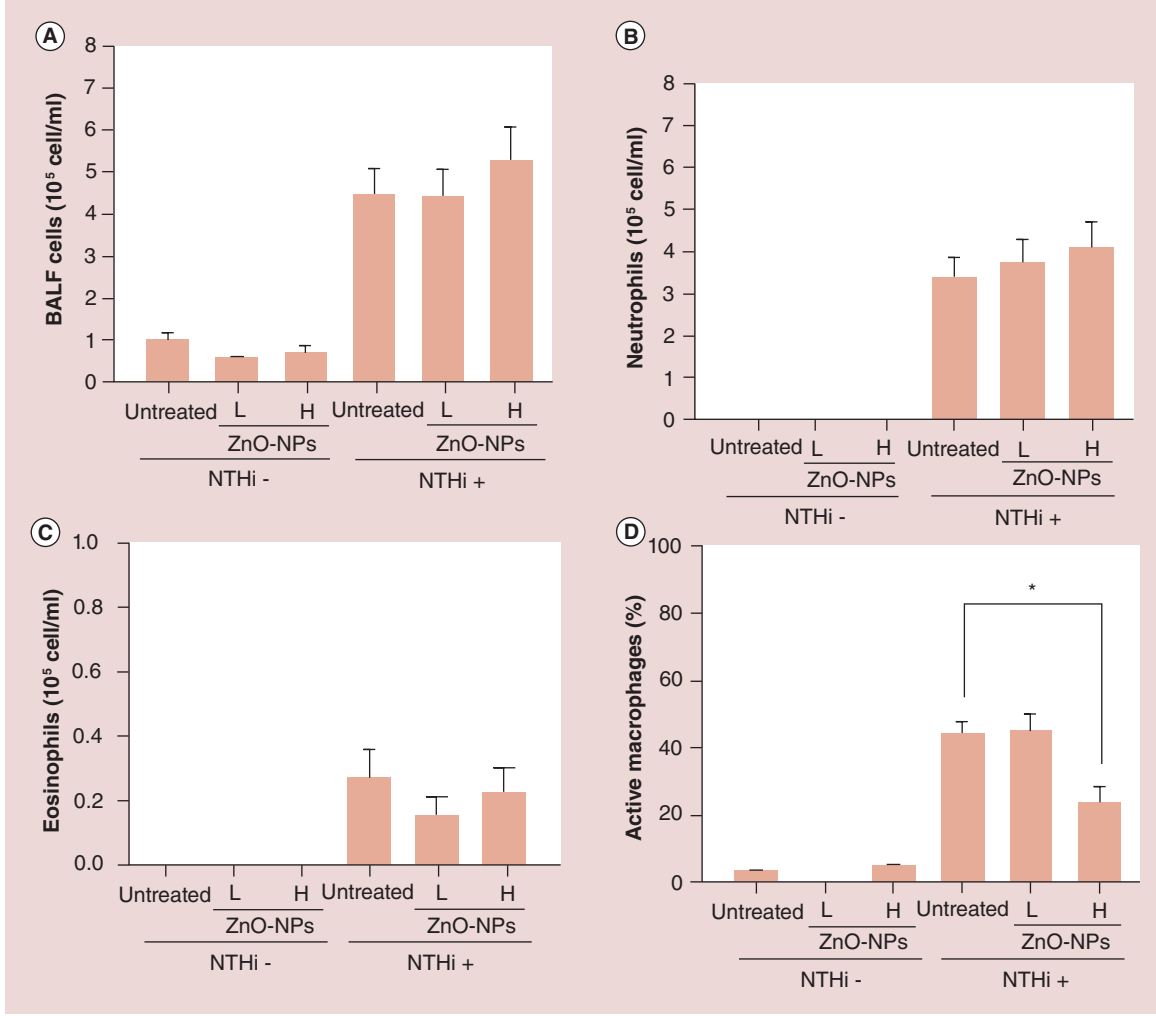

Figure 2. Zinc oxide nanoparticles suppress macrophage activation in response to nontypeable *Haemophilus influenzae* infection. Mice were exposed to particles for 14 days and infected or not infected with nontypeable *Haemophilus influenzae* for 4 h. After mice were sacrificed, bronchoalveolar lavage fluids were prepared for Wright–Giemsa staining. The following cell types were sorted and counted: **(A)** bronchoalveolar lavage fluid cells, **(B)** neutrophils, **(C)** eosinophils and **(D)** activated macrophages. p-values were determined using the Student's *t*-test. *$p < 0.05$.

H: High particle doses (140 μg/ml); L: Low particle doses (14 μg/ml); NTHi -: Noninfected with NTHi; NTHi +: Infected with nontypeable *Haemophilus influenzae*; ZnO-NP: ZnO nanoparticle.

showed dramatically decreased levels of iNOS mRNA in BALFs. These results indicate that ZnO-NPs may suppress the bacteria-induced iNOS-mediated inflammation pathway in macrophages.

ZnO-NPs attenuate phagocytosis of NTHi by macrophages

Because ZnO-NPs show cytotoxic and bactericidal activities via enhancing oxidative stress, which may cause cell apoptosis and disrupt bacterial outer membranes [17], we evaluated the cytotoxic and bactericidal effects of ZnO-NPs. RAW264.7 cells were treated with various concentrations of ZnO-NPs, and cell viability was analyzed using an MTT assay. When cells were treated with various concentrations of ZnO-NPs (1–10 μg/ml) for 24 h, cell and bacterial viability was scarcely influenced (Supplementary Figure 1). With increased concentrations, we observed that 100 μg/ml of ZnO-NPs had a slight bactericidal effect on NTHi and found that it causes 70% cell death (data not shown). Therefore, ZnO-NP concentrations less than 100 μg/ml (1, 5, 10 μg/ml) were selected to employ in our *in vitro* bacterial infection model.

To further investigate the effects of ZnO-NPs on innate sensing in response to bacterial infection, RAW264.7 cells were exposed to ZnO-NPs before being challenged with NTHi. Our data showed that treating cells with ZnO-NPs (10 μg/ml) enhanced NTHi extracellular survival (Figure 5A). However, levels of intracellular NTHi significantly decreased in cells treated with ZnO-NPs (Figure 5B). n addition, phagocytosis of FITC-NTHi by macrophages was markedly reduced in the presence of ZnO-NPs (Figure 5C). Our data again indicate that phagocytosis of NTHi and bacterial clearance by macrophages was mitigated by ZnO-NPs.

ZnO-NPs inhibit NTHi-induced NO production through the NF-κB signaling pathway

Because NTHi-induced iNOS expression in macrophages was suppressed by ZnO-NPs, we analyzed NO production by measuring nitrite levels. As shown in Figure 6A, the expression of cyclooxygenase 2 (COX-2) in NTHi-infected RAW264.7 cells was inhibited by treatment with ZnO-NPs. NTHi-induced NO production was decreased in a concentration-dependent manner in RAW264.7 cells upon treatment with ZnO-NPs (Figure 6B). In parallel, expression of iNOS mRNA was decreased by ZnO-NPs at concentrations of 1–10 μg/ml (Figure 6C).

We next investigated the effects of ZnO-NPs on levels of the transcription factor NF-κB, which plays a critical role in the regulation of iNOS expression [37]. The effects of ZnO-NPs on NF-κB expression

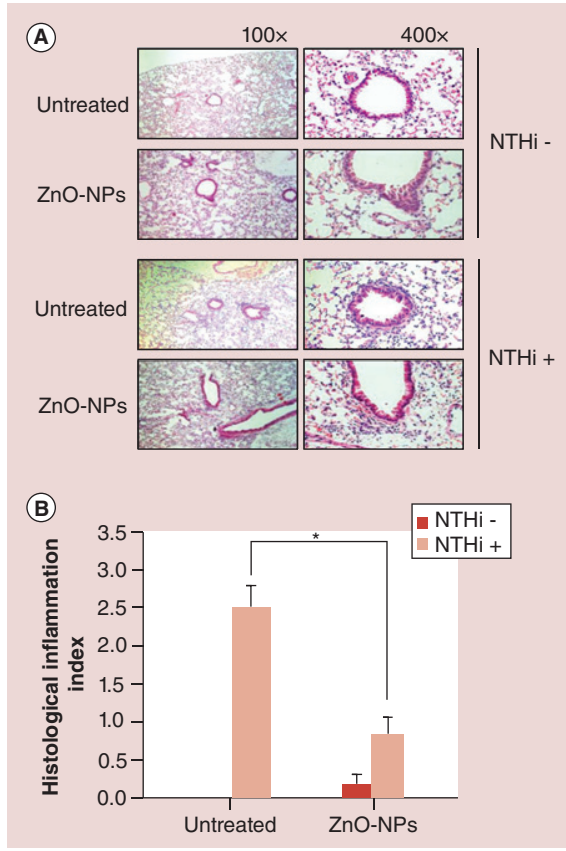

Figure 3. Zinc oxide nanoparticles inhibit nontypeable *Haemophilus influenzae*-induced lung inflammation. Mice were pretreated or not treated with zinc oxide nanoparticles (140 μg/ml), followed by infection or noninfection with nontypeable *Haemophilus influenzae*. **(A)** Lung sections were prepared for hematoxylin/eosin staining. **(B)** Quantification of the numbers of hematoxylin/eosin-stained cells is presented in the bar graphs.
*$p < 0.05$ compared with the untreated group.
NTHi -: Noninfected with nontypeable *Haemophilus influenzae*; NTHi +: Infected with NTHi; ZnO-NP: ZnO nanoparticle.

were then examined using the luciferase assay in RAW264.7 cells transfected with a NF-κB luciferase reporter. As shown in Figure 7A, in the absence of NTHi infection, ZnO-NPs alone did not alter the activation of the NF-κB promoter in macrophages. However, ZnO-NPs significantly inhibited NTHi-induced activation of the NF-κB promoter in a concentration-dependent manner. We then observed p65 localization, which was originally located in the cytosol before treatment of RAW264.7 cells with ZnO-NPs or NTHi (Figure 7B–C). After infection of cells with NTHi for 3 h, the yellow staining indicates that p65 (green) was translocated into the nucleus (red) of RAW264.7 cells. When cells were treated with ZnO-NPs followed by infection with NTHi, most of the p65 remained in the cytosol.

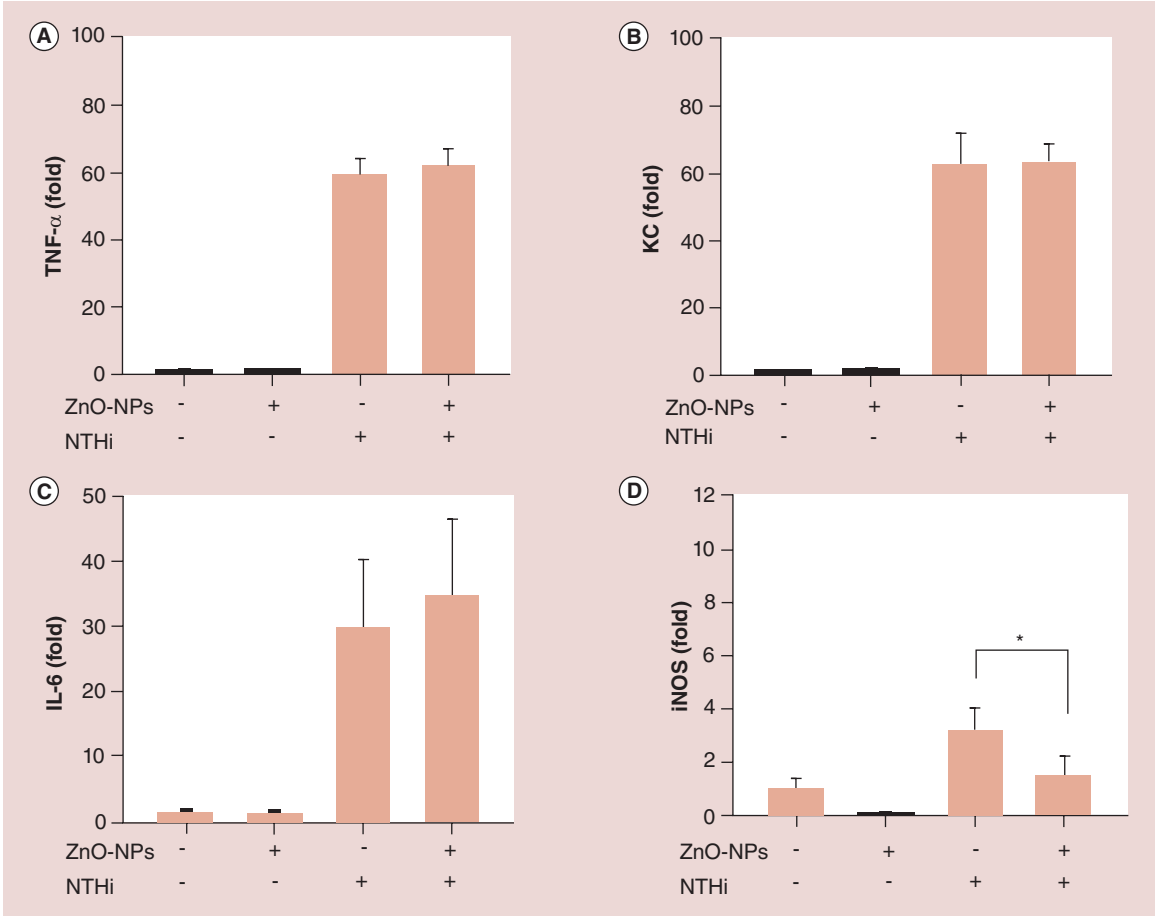

Figure 4. Zinc oxide nanoparticles inhibit nontypeable *Haemophilus influenzae*-induced inducible nitric oxide synthase mRNA expression in bronchoalveolar lavage fluid. Mice were treated or not treated with zinc oxide nanoparticles and infected or not infected with nontypeable *Haemophilus influenzae*. After mice were sacrificed, bronchoalveolar lavage fluids were prepared for cytokine assays to test for **(A)** TNF-α, **(B)** KC, **(C)** IL-6 or **(D)** iNOS mRNA expression level. Statistical significance was determined using the Student's *t*-test.
*$p < 0.05$.
KC: Keratinocyte-derived chemokine; NTHi: Nontypeable *Haemophilus influenzae*; ZnO-NP: ZnO nanoparticle.

Taken together, these results demonstrate that ZnO-NPs inhibit NTHi-stimulated NO production and iNOS expression in macrophages via triggering the NF-κB pathway.

Discussion

Absorption of NPs by a host can be mediated through inhalation, ingestion, dermal and parenteral routes [38]. Inhalation is the most common route and may affect the pulmonary immune system, which plays an important role in protection against pathogen infections [39]. Alveolar macrophages primarily responded to NPs, which were inhaled and remained in the lungs [40]. Additionally, macrophages are important to host defense against NTHi [41]. We established a nanoparticle-exposed mouse model and macrophages (RAW264.7) to assess the potential effects of ZnO-NPs on their ability to influence pulmonary immune activity in response to NTHi infection.

Absorption and tissue biodistribution of particles varies and mainly depends on particle size. In this study, ZnO-NPs enhanced NTHi survival not only in BALFs but also in lung tissue when compared with ZnO-MPs. This result corresponds with our previous findings that ZnO-NPs exhibited better absorption and wider tissue biodistribution than ZnO-MPs *in vivo* [14]. The organ biodistribution of ZnO-NPs that were administered by oral or intraperitoneal routes has been determined [14]. However, the biodistribution of NPs may differ between systemic administration and inhalation. Therefore, it is essential to evaluate the use of ZnO-NPs in living environments and to assess the tissue biodistribution of ZnO-NPs acquired through inhalation.

ZnO-NPs exhibit bactericidal activity and may kill bacteria by induction of reactive oxygen species (ROS), as has been reported previously [17]. However, the bactericidal effects of ZnONPs on NTHi have not yet

been elucidated. Our results showed that treatment of NTHi with ZnO-NPs (100 µg/ml) for 24 h only slightly affects bacterial viability. Comparing our findings with those of a previous study, which showed that exposure of bacteria to 81.4 µg/ml of ZnO-NPs could completely inhibit the growth of *Escherichia coli* [17], indicating that NTHi may have sophisticated mechanisms for enhancing resistance to ZnO-NPs. This finding could be supported by previous evidence that NTHi is able to degrade NO, which may lead to elevated bacterial survival [42]. Production of NO by macrophages is well-known to play pivotal roles in defense against bacterial infection [43,44]. In this study, exposure of macrophages to ZnO-NPs did not elevate NO production. In contrast, macrophages produced a significant level of NO in response to challenge by NTHi. Although we did not detect iNOS protein expression in the lungs, we suggest that ZnO-NPs might decrease NTHi-induced iNOS protein expression because they lower iNOS mRNA expression and reduce macrophage activation in the lungs. In addition, in the cell study, we found that ZnO-NPs decrease NTHi-induced NO production in activated macrophages (Figure 6). These results indicate that ZnO-NPs may influence NO-related pathways that subsequently suppress bacterial killing by macrophages. This finding corresponds with previous evidence that NO can mobilize zinc and affect zinc-related proteins [45], implying that ZnO-NPs may consume NO, thus protecting pathogens from eradication.

Previous studies have indicated that, in addition to physiochemical characteristics, zinc ion (Zn^{2+}) plays a significant role in ZnO-NP-induced cytotoxicity [46,47]. In contrast, in another study, the authors reported that Zn^{2+} is not involved in ZnO-NP-induced cytotoxicity [48]. In the present study, to

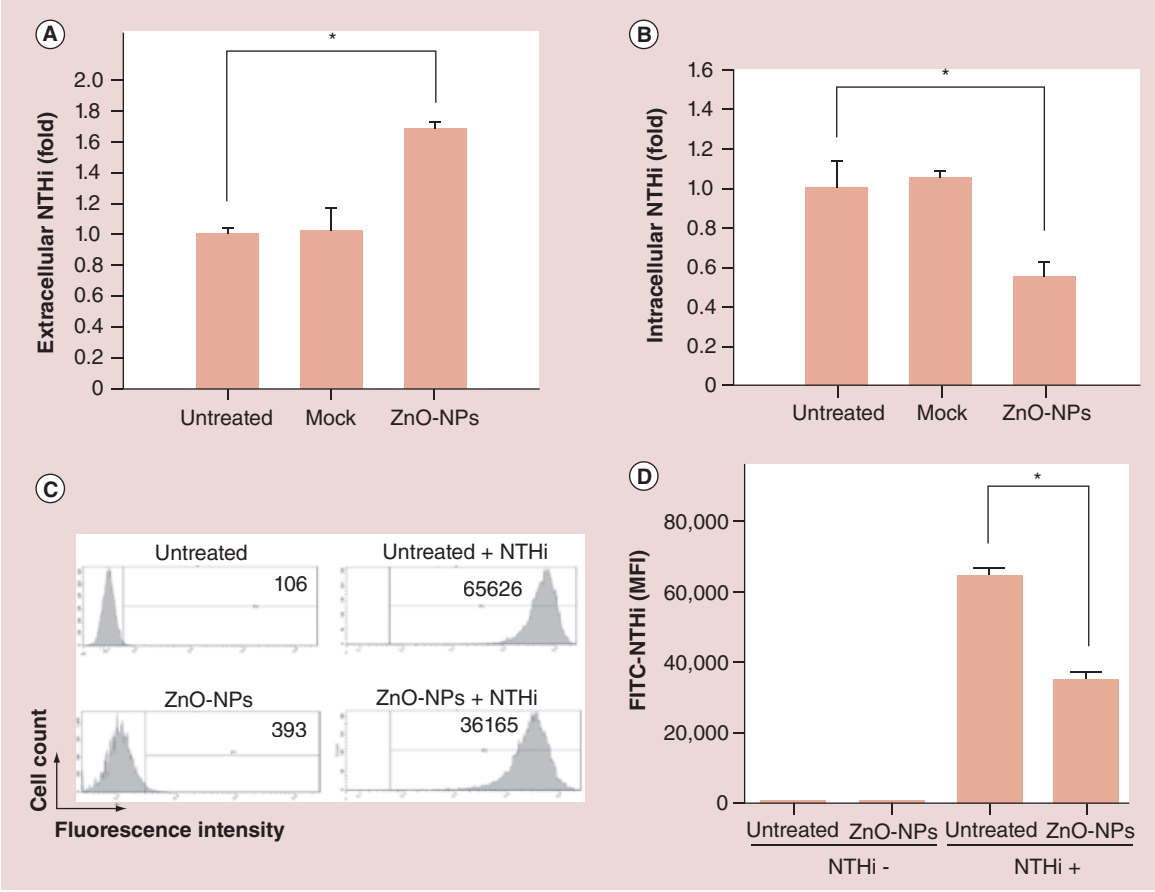

Figure 5. Zinc oxide nanoparticles impair bacterial clearance by macrophages. RAW264.7 cells were sham-exposed (untreated) or exposed to zinc oxide nanoparticles (10 µg/ml) prior to infection with nontypeable *Haemophilus influenzae* at a multiplicity of infection of 100 for 3 h with nontypeable *Haemophilus influenzae*. **(A)** Extracellular survival, **(B)** intracellular survival and **(C)** phagocytosis by macrophages were determined as described in the 'Materials & methods' section.
*$p < 0.05$ compared with the untreated group.
FITC: Fluorescein isothiocyanate-conjugated NTHi; MFI: Mean fluorescence intensity; NTHi: Nontypeable *Haemophilus influenzae*; NTHi -: Noninfected with nontypeable *Haemophilus influenzae*; NTHi +: Infected with NTHi; ZnO-NP: ZnO nanoparticle.

clarify this important issue, we detected the concentration of Zn^{2+} in the culture medium. As shown in Supplementary Table 1, we detected Zn^{2+} in RPMI medium containing 10% FBS in a range of 2000 mg/ml to 0.003 mg/ml of ZnO-NPs and ZnO-MPs. We found that the maximal Zn^{2+} concentration in the medium was approximately 1.3 μg/ml and plateaued at 0.003 mg/ml ZnO-NPs. The inhibitory effects of macrophage function did not show a dose-dependent increase with elevated Zn^{2+} concentration. In addition, we found that Zn^{2+} concentration in ZnO-MPs showed a similar concentration but did not exhibit inhibitory effects on macrophage activation. Therefore, the conclusion that ZnO-NPs likely inhibit macrophage activation is mainly attributed to ZnO-NPs rather than the concentration of the released zinc ion.

Conclusion

In this study, we established cell and animal models to demonstrate that inhalation of ZnO-NPs impaired NO production and macrophage activation, leading to delayed pathogen clearance. We further revealed that ZnO-NPs inhibited NTHi-stimulated NO production via triggering the NF-κB pathway in macrophages. Our findings indicate that exposure to ZnO-NPs may lead to increased risk for human health, particular in pulmonary infections, by attenuating host immune responses against bacteria.

Future perspective

ZnO-NPs have been used widely in human living environments and the possible toxic effects on human health have raised serious concerns. In this study, inhalation of ZnO-NPs impaired macrophage activation, leading to attenuation of NTHi clearance in a mouse infection model. Our results revealed that ZnO-NPs inhibited NTHi-stimulated NO production via triggering the NF-κB pathway in macrophages. Future work is warranted to investigate the toxicological relevance of ZnO-NPs in the respiratory airway, particularly with respect to host defense against bacterial infection in human.

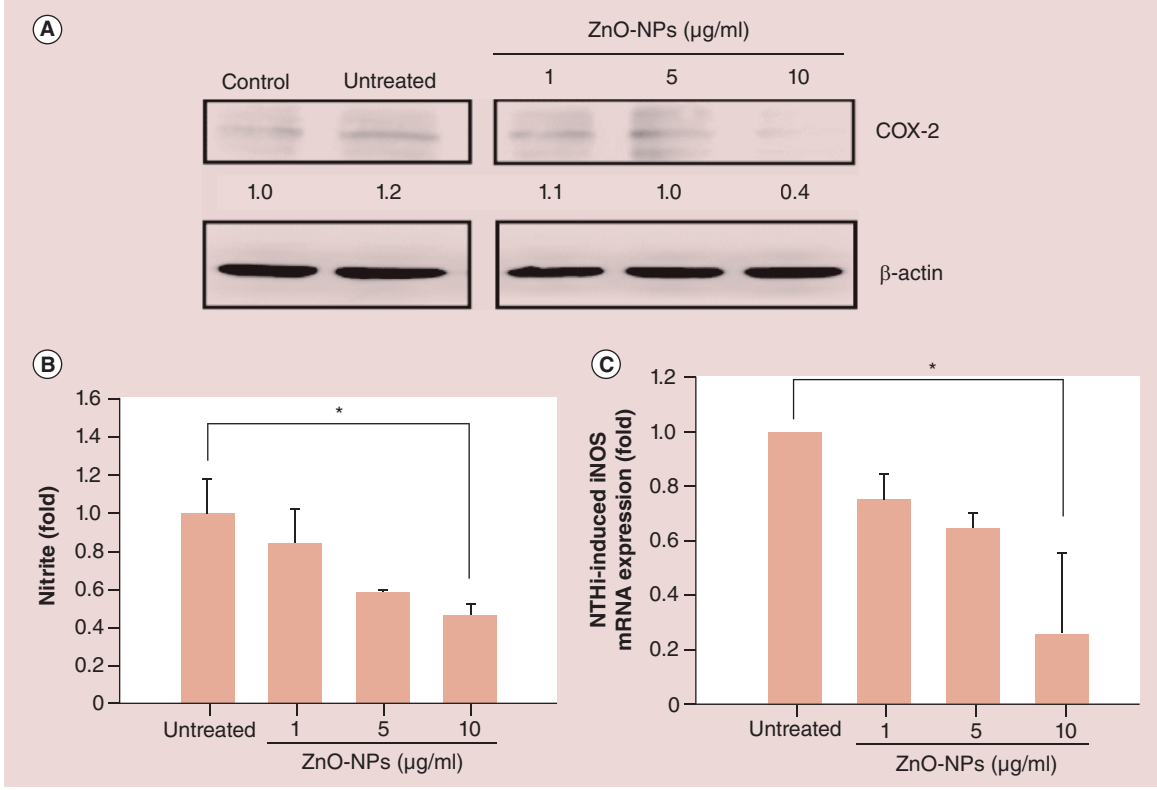

Figure 6. Effect of zinc oxide nanoparticles on nontypeable *Haemophilus influenzae*-induced nitric oxide production by macrophages. RAW264.7 cells were treated with various concentrations of ZnO-NPs for 3 h followed by infection with NTHi at a MOI of 100 for 3 h. **(A)** Cell lysates were prepared to assess COX-2 protein expression by Western blot. Protein expression levels were quantified for signal intensity; normalization to β-actin is indicated at the bottom of each lane. **(B)** Nitrite levels of culture supernatants were determined using the Griess reagent. **(C)** iNOS mRNA expression was analyzed using quantitative real-time PCR and GAPDH was used as an internal control.
*$p < 0.05$ compared with the untreated group.
ZnO-NP: ZnO nanoparticle.

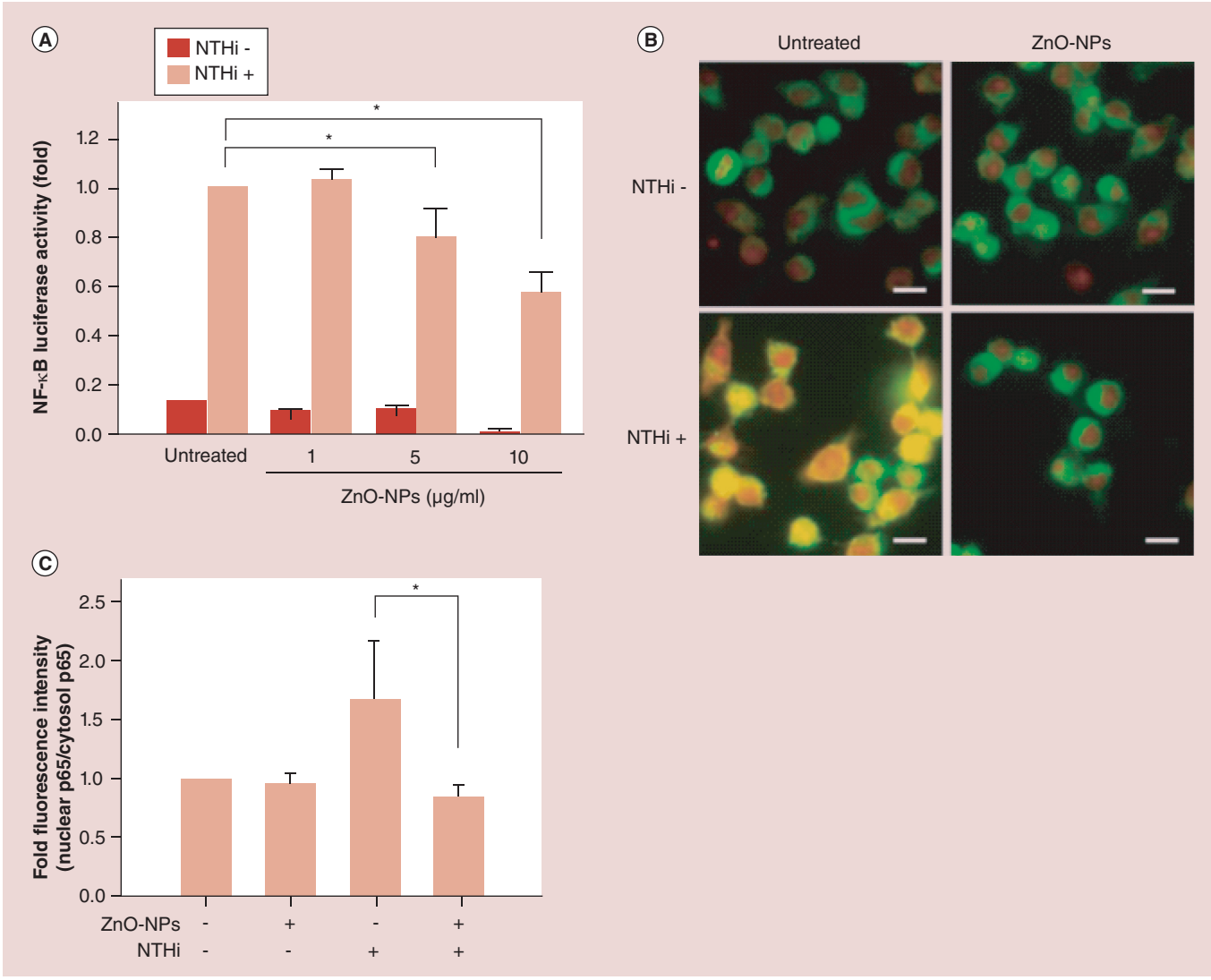

Figure 7. Zinc oxide nanoparticles attenuate NF-κB activation in response to nontypeable *Haemophilus influenzae* infection.
(A) RAW264.7 cells transfected with NF-κB reporter or β-Gal-lacZ (1 μg each) were exposed to ZnO-NPs and infected with or without NTHi at a multiplicity of infection of 100. Luciferase activity was normalized to the expression level of β-Gal-lacZ. **(B)** Cells were probed with anti-p65 followed by Alexa Fluor® 488-conjugated goat anti-mouse IgG (green) and propidium iodide to visualize the nucleus (red). Yellow in the merged images indicates colocalization of p65 and the nucleus. **(C)** The nuclear translocation of phosphorylated p65 was analyzed using confocal microscopy. Scale bars: 10 μm. Statistical significance was evaluated using the Student's *t*-test.
*$p < 0.05$.
NTHi: Nontypeable *Haemophilus influenzae*; ZnO-NP: ZnO nanoparticle.

Acknowledgements

The authors would like to thank Mei-Zi Huang for expert technical assistance. Confocal microscopy was performed through the use of the microscopic facility at the Scientific Instrument Center of Academia Sinica and with the assistance of Shu-Chen Shen.

Financial & competing interests disclosure

This work was supported by the National Science Council (grant no. NSC101-2313-B-039-004-MY3, NSC102-2314-B-039-016 and NSC102-2633-B-039-001), China Medical University, Taiwan (grant no. CMU102-S-27 and CMU102-S-28), Taiwan Ministry of Health and Welfare Clinical Trial, the Research Center for Excellence (grant no. DOH103-TD-B-111-004), and the Tomorrow Medicine Foundation. The authors have no other relevant affiliations or financial involvement with any organization or entity with a financial interest in or financial conflict with the subject matter or materials discussed in the manuscript apart from those disclosed.

No writing assistance was utilized in the production of this manuscript.

Executive summary

Background

- Inhalation of nanoparticles (NPs) via the respiratory tract may induce immune-suppressive effects, impairing macrophage functions and attenuating host defenses against bacterial infection.
- How zinc oxide nanoparticles (ZnO-NPs) affect the host pulmonary immune system's response to nontypeable *Haemophilus influenzae* (NTHi) infection was investigated.

Materials & methods

- A ZnO-NP-exposed mouse model, which was challenged with NTHi, was established to evaluate pulmonary immune responses and lung bacterial clearance.
- The effect of ZnO-NPs on triggering signalling molecules, which may lead to attenuation of pulmonary immune activation in response to NTHi infection, was investigated.

Results

- Inhalation of high concentrations of ZnO-NPs reduced bacterial clearance in the murine pulmonary system.
- The phagocytosis of NTHi and bacterial clearance by macrophages was mitigated by ZnO-NPs.
- ZnO-NPs inhibit NTHi-stimulated NO production and iNOS expression in macrophages via triggering the NF-κB pathway.

Conclusion

- Our findings indicate that exposure to ZnO-NPs may lead to increased risk for human health, particularly in pulmonary infections, by attenuating the host's immune responses against bacteria.

References

Papers of special note have been highlighted as: •• of considerable interest

1 Liang M, Guo LH. Application of nanomaterials in environmental analysis and monitoring. *J. Nanosci. Nanotechnol.* 9(4), 2283–2289 (2009).

2 Stensberg MC, Wei Q, McLamore ES *et al.* Toxicological studies on silver nanoparticles: challenges and opportunities in assessment, monitoring and imaging. *Nanomedicine (Lond.)* 6(5), 879–898 (2011).

3 Klaine SJ, Alvarez PJ, Batley GE *et al.* Nanomaterials in the environment: behavior, fate, bioavailability, and effects. *Environ. Toxicol. Chem.* 27(9), 1825–1851 (2008).

4 Faunce T, Watal A. Nanosilver and global public health: international regulatory issues. *Nanomedicine (Lond.)* 5(4), 617–632 (2010).

5 Oberdorster G, Maynard A, Donaldson K *et al.* Principles for characterizing the potential human health effects from exposure to nanomaterials: elements of a screening strategy. *Part. Fibre Toxicol.* 2(8), 1–35 (2005).

6 Wang H, Du LJ, Song ZM *et al.* Progress in the characterization and safety evaluation of engineered inorganic nanomaterials in food. *Nanomedicine (Lond.)* 8(12), 2007–2025 (2013).

•• **Provides evidence that the risk for human health of inorganic nanomaterials in food.**

7 Aydin Sevinc B, Hanley L. Antibacterial activity of dental composites containing zinc oxide nanoparticles. *J. Biomed. Mater. Res. B. Appl. Biomater.* 94(1), 22–31 (2010).

8 Leite-Silva VR, Le Lamer M, Sanchez WY *et al.* The effect of formulation on the penetration of coated and uncoated zinc oxide nanoparticles into the viable epidermis of human skin *in vivo*. *Eur. J. Pharm. Biopharm.* 84(2), 297–308 (2013).

9 Barkalina N, Charalambous C, Jones C *et al.* Nanotechnology in reproductive medicine: emerging applications of nanomaterials. doi:10.1016/j.nano.2014.01.001 *Nanomedicine* (2014) (Epub ahead of print).

10 Gulson B, Wong H, Korsch M *et al.* Comparison of dermal absorption of zinc from different sunscreen formulations and differing UV exposure based on stable isotope tracing. *Sci. Total Environ.* 420, 313–318 (2012).

11 Gulson B, McCall M, Korsch M *et al.* Small amounts of zinc from zinc oxide particles in sunscreens applied outdoors are absorbed through human skin. *Toxicol. Sci.* 118, 140–149 (2010).

12 Monteiro-Riviere NA, Baroli B. Nanomaterial penetration. *Toxicol. Skin* 333–346 (2010).

13 Lademann J, Weigmann H, Rickmeyer C *et al.* Penetration of titanium dioxide microparticles in a sunscreen formulation into the horny layer and the follicular orifice. *Skin Pharmacol. Appl. Skin Physiol.* 12(5), 247–256 (1999).

14 Li CH, Shen CC, Cheng YW *et al.* Organ biodistribution, clearance, and genotoxicity of orally administered zinc oxide nanoparticles in mice. *Nanotoxicology* 6(7), 746–756 (2012).

•• **Breakthrough study providing evidence that oral administration and intraperitoneal injection of ZnO-NPs resulted in their absorption into the circulatory system, followed by biodistribution to the liver, spleen and kidney.**

15 Osmond-McLeod MJ, Osmond RI, Oytam Y *et al.* Surface coatings of ZnO nanoparticles mitigate differentially a host of transcriptional, protein and signalling responses in primary human olfactory cells. *Part. Fibre Toxicol.* 10(1), 54 (2013).

16 Li CH, Liao PL, Shyu MK *et al.* Zinc oxide nanoparticles-induced intercellular adhesion molecule 1 expression requires Rac1/Cdc42, mixed lineage kinase 3, and c-Jun N-terminal kinase activation in endothelial cells. *Toxicol. Sci.* 126(1), 162–172 (2012).

17 Padmavathy N, Vijayaraghavan R. Interaction of ZnO nanoparticles with microbes – a physio and biochemical assay. *J. Biomed. Nanotechnol.* 7(6), 813–822 (2011).

18 Matsumura M, Takasu N, Nagata M *et al.* Effect of ultrafine zinc oxide (ZnO) nanoparticles on induction of oral tolerance in mice. *J. Immunotoxicol.* 7(3), 232–237 (2010).

19 Hackenberg S, Scherzed A, Technau A *et al.* Cytotoxic, genotoxic and pro-inflammatory effects of zinc oxide nanoparticles in human nasal mucosa cells *in vitro*. *Toxicol. In vitro* 25(3), 657–663 (2011).

20 Faden H, Duffy L, Williams A *et al.* Epidemiology of naso-pharyngeal colonization with nontypeable *Haemophilus influenzae* in the first 2 years of life. *J. Infect. Dis.* 172(1), 132–135 (1995).

•• **Provides the epidemiology and pathogenesis of nontypeable *Haemophilus influenzae* infection in human.**

21 Murphy TF, Bakaletz LO, Smeesters PR. Microbial interactions in the respiratory tract. *Pediatr. Infect. Dis. J.* 28(10 Suppl.), S121–S126 (2009).

22 Rao VK, Krasan GP, Hendrixson DR *et al.* Molecular determinants of the pathogenesis of disease due to non-typable *Haemophilus influenzae*. *FEMS Microbiol. Rev.* 23(2), 99–129 (1999).

23 Bandi V, Apicella MA, Mason E *et al.* Nontypeable *Haemophilus influenzae* in the lower respiratory tract of patients with chronic bronchitis. *Am. J. Respir. Crit. Care Med.* 164(11), 2114–2119 (2001).

24 St Geme JW 3rd. The pathogenesis of nontypable *Haemophilus influenzae* otitis media. *Vaccine* 19(Suppl. 1), S41–S50 (2000).

25 Berenson CS, Garlipp MA, Grove LJ *et al.* Impaired phagocytosis of nontypeable *Haemophilus influenzae* by human alveolar macrophages in chronic obstructive pulmonary disease. *J. Infect. Dis.* 194(10), 1375–1384 (2006).

26 Sethi S, Evans N, Grant BJ *et al.* New strains of bacteria and exacerbations of chronic obstructive pulmonary disease. *N. Engl. J. Med.* 347(7), 465–471 (2002).

27 Lee CC, Lai YT, Chang HT *et al.* Inhibition of high-mobility group box 1 in lung reduced airway inflammation and remodeling in a mouse model of chronic asthma. *Biochem. Pharmacol.* 86(7), 940–949 (2013).

28 Lee CC, Wang CN, Kang JJ *et al.* Antiallergic asthma properties of brazilin through inhibition of Th2 responses in T cells and in a murine model of asthma. *J. Agric. Food Chem.* 60(37), 9405–9414 (2012).

29 Lee CC, Liao JW, Kang JJ. Motorcycle exhaust particles induce airway inflammation and airway hyperresponsiveness in BALB/C mice. *Toxicol. Sci.* 79(2), 326–334 (2004).

30 Poje G, Redfield RJ. General methods for culturing *Haemophilus influenzae*. *Methods Mol. Med.* 71, 51–56 (2003).

31 Lai CK, Lu YL, Hsieh JT *et al.* Development of chitosan/heparin nanoparticle-encapsulated cytolethal distending toxin for gastric cancer therapy. *Nanomedicine (Lond.)* 9(6), 803–807 (2013).

32 Lien HM, Wang CY, Chang HY *et al.* Bioevaluation of *Anisomeles indica* extracts and their inhibitory effects on *Helicobacter pylori*-mediated inflammation. *J. Ethnopharmacol.* 145(1), 397–401 (2013).

33 Lai CH, Chang YC, Du SY *et al.* Cholesterol depletion reduces *Helicobacter pylori* CagA translocation and CagA-induced responses in AGS cells. *Infect. Immun.* 76(7), 3293–3303 (2008).

34 Lu DY, Tang CH, Chang CH *et al.* *Helicobacter pylori* attenuates lipopolysaccharide-induced nitric oxide production by murine macrophages. *Innate Immun.* 18(3), 406–417 (2012).

35 Lu DY, Chen HC, Yang MS *et al.* Ceramide and Toll-like receptor 4 are mobilized into membrane rafts in response to *Helicobacter pylori* infection in gastric epithelial cells. *Infect. Immun.* 80(5), 1823–1833 (2012).

36 Lai CH, Wang HJ, Chang YC *et al.* *Helicobacter pylori* CagA-mediated IL-8 induction in gastric epithelial cells is cholesterol-dependent and requires the C-terminal tyrosine phosphorylation-containing domain. *FEMS Microbiol. Lett.* 323(2), 155–163 (2011).

37 Marks-Konczalik J, Chu SC, Moss J. Cytokine-mediated transcriptional induction of the human inducible nitric oxide synthase gene requires both activator protein 1 and nuclear factor kappaB-binding sites. *J. Biol. Chem.* 273(35), 22201–22208 (1998).

38 Stern ST, McNeil SE. Nanotechnology safety concerns revisited. *Toxicol. Sci.* 101(1), 4–21 (2008).

39 Gordon T, Chen LC, Fine JM *et al.* Pulmonary effects of inhaled zinc oxide in human subjects, guinea pigs, rats, and rabbits. *Am. Ind. Hyg. Assoc. J.* 53(8), 503–509 (1992).

40 Oberdorster G, Sharp Z, Atudorei V *et al.* Extrapulmonary translocation of ultrafine carbon particles following whole-body inhalation exposure of rats. *J. Toxicol. Environ. Health. A* 65(20), 1531–1543 (2002).

41 Noel GJ, Hoiseth SK, Edelson PJ. Type B capsule inhibits ingestion of *Haemophilus influenzae* by murine macrophages: studies with isogenic encapsulated and unencapsulated strains. *J. Infect. Dis.* 166(1), 178–182 (1992).

42 Harrington JC, Wong SM, Rosadini CV *et al.* Resistance of *Haemophilus influenzae* to reactive nitrogen donors and gamma interferon-stimulated macrophages requires the formate-dependent nitrite reductase regulator-activated *ytfE* gene. *Infect. Immun.* 77(5), 1945–1958 (2009).

43 Fang FC. Perspectives series: host/pathogen interactions. Mechanisms of nitric oxide-related antimicrobial activity. *J. Clin. Invest.* 99(12), 2818–2825 (1997).

44 Maa MC, Leu TH. Activation of Toll-like receptors induces macrophage migration via the iNOS/Src/FAK pathway. *BioMedicine* 1(1), 11–15 (2011).

45 Schapiro JM, Libby SJ, Fang FC. Inhibition of bacterial DNA replication by zinc mobilization during nitrosative stress. *Proc. Natl Acad. Sci. USA* 100(14), 8496–8501 (2003).

•• **Demonstrates DNA-binding zinc metalloproteins as critical targets of nitric oxide-related antimicrobial activity.**

46 Kao YY, Chen YC, Cheng TJ *et al.* Zinc oxide nanoparticles interfere with zinc ion homeostasis to cause cytotoxicity. *Toxicol. Sci.* 125(2), 462–472 (2012).

47 Fukui H, Horie M, Endoh S *et al.* Association of zinc ion release and oxidative stress induced by intratracheal instillation of ZnO nanoparticles to rat lung. *Chem. Biol. Interact.* 198(1–3), 29–37 (2012).

48 Moos PJ, Chung K, Woessner D *et al.* ZnO particulate matter requires cell contact for toxicity in human colon cancer cells. *Chem. Res. Toxicol.* 23(4), 733–739 (2010).